The Structural Conjugate Heat Transfer Solver - Recent Developments

Thomas Klöppel

DYNAmore GmbH, Stuttgart, Germany

Abstract

It is the objective of this contribution to present and discuss recent developments in the structural conjugate heat transfer solver in LS-DYNA to be used mainly for the thermo-mechanical coupled simulation of complex manufacturing processes such as for example hot forming, heat treatment and welding. Beside the multi-physics nature the complexity of these processes is due to the usually challenging constitutive behavior of the employed materials.
In the next section some of the thermo-mechanical material models in LS-DYNA are briefly discussed and recent modifications and enhancements to those models are shown. Furthermore, the new material ***MAT_GENERALIZED_PHASECHANGE** (***MAT_254**) is introduced, which features a very flexible and widely applicable modelling approach for phase change kinematics.
The paper also addresses two new options for the thermal contact. First of all, heat transfer between a shell edge and a surface (either shell or solid face) can now be considered. Second, a special welding contact formulation has been implemented. Above a certain temperature, the formulation switches from a sliding to a tied formulation and uses different parameters for the heat transfer. Although both modifications have been motivated by welding applications, they have also proven to be helpful for other applications.
The presentation of a new heat source boundary condition in the fourth section completes this work's list of developments. It is defined with the keyword ***BOUNDARY_THERMAL_WELD_TRAJECTORY** and allows modelling of a moving heat source for coupled and thermal-only simulations and provides a very flexible input for the shape of the heat source.

Material Formulations for Hot Forming and Welding

If the user is mainly interested in the deflection of the part after a welding stage and if the resulting microstructure is thought to play only a secondary role, the LS-DYNA material ***MAT_CWM** (***MAT_270**) is a suitable choice to model the welded parts as well as filler material that is commonly used in welding processes, as has been demonstrated in [1]**.**
Nevertheless, the objective of many welding and almost all hot-forming and heat treatment simulations is the prediction of the phase transformations within the material and hence of the resulting material properties. The LS-DYNA materials ***MAT_UHS_STEEL** (***MAT_244**) and ***MAT_PHS_BMW** (***MAT_248**) possess phase transformation models tailored for ultra-high strength steel alloys in a press hardening process. For details on ***MAT_244** see [2], [3]; on ***MAT_248** see [4], [5] . Some recent modifications on material ***MAT_244** in order to widen its range of applications and improve the stability are presented in the next subsection.
The algorithmic parameters of the material formulations mentioned above are based on the chemical composition of the material. This enables a relatively simple input, but restricts the application of the model to only a few steel alloys. The second subsection introduces the recently implemented material ***MAT_GENERALIZED_PHASECHANGE** (***MAT_254**) that has been implemented in order to provide a suitable model for a wide range of metals, particularly in terms of phase kinetics.

2.1 Work on existing material models

For ultra-high strength steel alloys the LS-DYNA material ***MAT_244**, which is based on the work of Åkerström et al. [2], [3] is a suitable choice. The formulation expects the input of the chemical composition and the thermo-mechanical properties of the individual phases of the microstructure. The mechanical response of the material is then determined using a linear mixture rule in terms of the current phase contents.
Within the last two or three years the implementation of the phase change model has been revised in order to increase the stability and applicability. The starting temperatures for the micro-structure transformations can now be chosen for both heating and cooling individually. Furthermore, transformation induced strains are considered. In dilatometer experiments these show as

characteristic jumps in strain over temperature curves. The height of the jumps varies with temperature and naturally with the phase combinations. This information about the jumps can serve as input in form of tabular data. As Fig. 1 demonstrates the revised material can capture these jumps between different dilatometer curves for the individual phases.

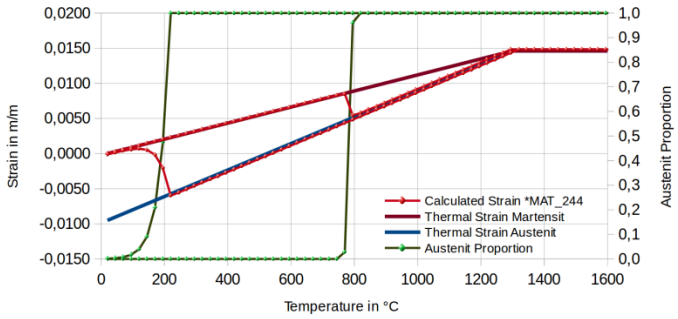

Fig.1: The effect of transformation induced strains: Dilatometer experiment and numerical simulation

To be applicable to welding simulations, in which temperatures might locally exceed the melting temperature, an annealing functionality (as known from ***MAT_270**) is needed. Above a certain limiting temperature, history variables such as effective plastic strain and back stresses are re-initialized. The material will show an ideal plastic flow behavior but does not accumulate internal plasticity data.
For many line-welding processes material is added during the process and it is often desirable to use for the same material for the filler as for the welded parts. Consequently, the material formulation has to account for two different states: until its activation by the weld torch it is in a ghost state, thereafter it is in the solid state as the welded structure. In the ghost state, the material is characterized by negligible thermal and mechanical properties. This reflects the fact that in the real process the filler material is added to the weld seam at the same time the weld torch reaches the specific region. Algorithmically, activation occurs within a certain temperature range, in which the material parameters are linearly interpolated between ghost and solid properties. Details on this modelling technique can be found in Lindström [6]. For a validation against experimental data the reader is referred to Lindström et al. [7]. Information on enhancements in ***MAT_244** can be found in [8].

2.2 A new material model for multi-phase metals

As the range of application of the available models is restricted only to UHS steel alloys, the main objective of the new implementation is to provide a suitable material formulation for a large range of metals used in welding and heat treatment applications. Therefore, the LS-DYNA material ***MAT_GENERALIZED_PHASECHANG** (**MAT_254**) accounts for up to 24 phases and it is important to note that the phases are not hard-coded to represent a certain microstructure phase. The user has to decide which of the possible phase transformations is to be considered and what transformation law from a list of well-established transformation laws is most suitable for the respective transformation. Each of the models requires a different set of parameters. Naturally, such a generic approach provides great flexibility, but goes along with a more complex material parameterization.
The thermo-mechanical formulation itself is similar to what can be found in other LS-DYNA constitutive models: the material features a von-Mises plasticity depending on temperature, strain rate and phase concentrations. Young's modulus, Poisson's ratio, and coefficient of thermal expansion can be given as functions of phase and temperature. From the micro-structure composition, the thermo-mechanical properties are calculated using a possibly temperature dependent linear mixture rule.
Reset of history data for the plasticity algorithm is an important effect the material has to capture to be applicable to welding simulations and it has hence been incorporated into the new material. On the other hand, the material formulation does not necessitate a distinguished ghost state since inactive material can just be identified with one of the microstructure phases that is transformed into an active phase during heating.
For the calculations of the micro-structure evolution a new concept has been implemented. Phase changes are controlled by a two-dimensional transformation matrix, where the first dimension is the base phase and the second the generated phase. This implies that for any phase to be transformed a load curve is specified in the ***DEFINE_TABLE(_2D)**. The load curve defines the phase transformation law as function of the resulting phase. For any of the defined transformations starting and end temperature have to be defined and have to be given in the same matrix form.

In the current state of the implementation four different micro-structure models are accounted for. If the phase transformation laws 1 (cooling) or -1 (heating) are chosen in the respective load curve, the so-called Koistinen-Marburger model, see [9], is used. It is widely accepted for diffusionless processes. It calculates the generated phase concentration x_b as function of the current temperature T and the transformed phase x_a using the formula

$$x_b = x_a\left(1.0 - e^{-\alpha\,\kappa\,(T_{start}-T)}\right). \tag{1}$$

In this equation the parameter κ is 1.0 for cooling and -1.0 for heating. Equation (1) requires only the scalar-valued Koistinen-Marburger factor α as input.
The second model implements one of the most widely used diffusive phase transformations laws: the extended Johnson-Mehl-Avrami-Kolmogorov (JMAK), see for example review in [10]. Based on an temperature depending equilibrium concentration $x_{eq}(T)$ and a relaxation time $\tau(T)$ the differential form

$$\frac{dx_b}{dt} = n(T)(k_{ab}x_a - k'_{ab}x_b)\left(\ln\left(\frac{k_{ab}(x_a + x_b)}{k_{ab}x_a - k'_{ab}x_b}\right)\right)^{\frac{n(T)-1.0}{n(T)}} \tag{2}$$

with parameters $k_{ab} = \frac{x_{eq}(T)}{\tau(T)} f(\dot{T}), k'_{ab} = \frac{1.0-x_{eq}(T)}{\tau(T)} f'(\dot{T})$

defines the transformation from x_a to x_b. The functions $f(\dot{T})$ and $f'(\dot{T})$ are correction functions accounting for temperature rate effects. For a constant exponent $n(T) = 1$ equation (2) reduces to the so-called Leblond model [11]. The model is applicable for heating and cooling. It requires the input of the temperature or temperature rate dependent parameters $n, x_{eq}, \tau, f, \dot{f}$.
The last two models haven been implemented because they are the base of microstructure evolution in ***MAT_UHS_STEEL**. For cooling, the model proposed by Kirkaldy and Venugopalan [12] can be employed for diffusive transformations. In contrast to the previous models the evolution equations here also depend on the grain size. Finally, the phase kinetics in ***MAT_UHS_STEEL** during heating is governed by the model of Oddy et al. [13]. It has been added to ***MAT_GENERALIZED_PHASECHANGE** as model -4. For details on these models and necessary input the user is referred to [14].
As discussed above, phase transition between ferritic and austenitic phases goes along with transformation induced strains. This effect is also accounted for by the new material model. It is important to note that the effect adds significant non-linearities with respect to the temperature to the material. Welding simulations usually feature locally high temperature rates and temperature gradients due to the high power of typical heat sources. Therefore, using a reasonably large time step with respect to simulation time will lead to a temperature increase of several hundred Kelvin at some nodes within one time step. The strain results for one rapidly heated element are shown in Fig. 2. The obtained curves for a large time step (B) and a very small time step (C) deviate significantly, since the transformation induced strains cannot correctly by resolved in time in case of large time step sizes.

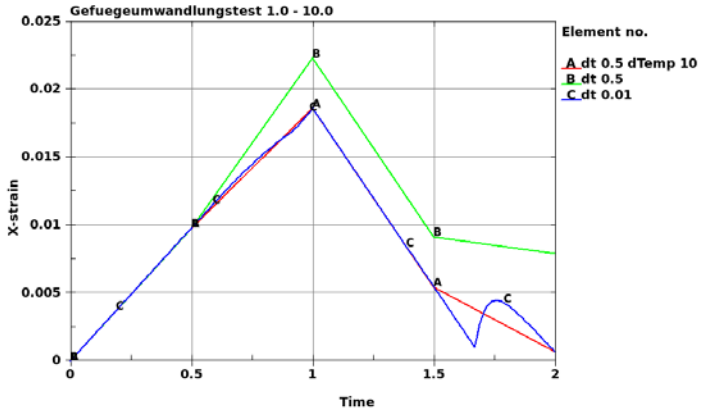

Fig.2: The effect of different time step sizes and subcycling.

Therefore, an input parameter representing the maximum temperature increase within one time step that is expected to show acceptable results has been added. If the temperature increase is too large in one integration point, a sub-cycling procedure is invoked assuming a constant temperature rate within one thermal time step. The quality of the strain results can be significantly improved by this approach as curve (A) in Fig. 2 shows. As the sub-cycling is only done at certain regions, the simulation time is only mildly affected for realistic examples.
Phase transformations do not only induce elastic but also plastic strains. The algorithm to calculate the transformation induced plasticity (TRIP) is based on the formulation proposed by Leblond [15]. This formulation has a very high impact on the residual stress distribution of welded structures and can be activated by defining a non-zero value for the parameter TRIP.

New Contact Options

This section introduces two newly developed contact algorithms in LS-DYNA. The implementations have been motivated by computational welding mechanics, but are general enough to be helpful in other thermo-mechanical coupled applications as well.

3.1 Shell edge thermal contact

Process simulations in manufacturing industries and in particular in automotive usually use shell discretizations or discretizations with both shell and solid elements. The standard thermal contact algorithms in LS-DYNA require a surface-to-surface type contact. Consequently, simulations of heat transfer in a T-joint modelled with shell elements or in a connection of a shell edge to a solid as it frequently occurs in welding simulations (connection of a blank to filler material in a weld seam) have required the development of a new contact option.
The new implementation has only be possible because LS-DYNA features a thermal thick shell formulation with bi-linear in-plane shape functions and a quadratic temperature shape function across the thickness of the shell. For this formulation virtual nodes are created at bottom and top of the shell element which can be used to reconstruct the three-dimensional geometry at the shell edges. If the parameter **ALGO** in the thermal contact card is set to 2 (two-way) or 3 (one-way), the reconstructed geometry is used for the contact algorithm.

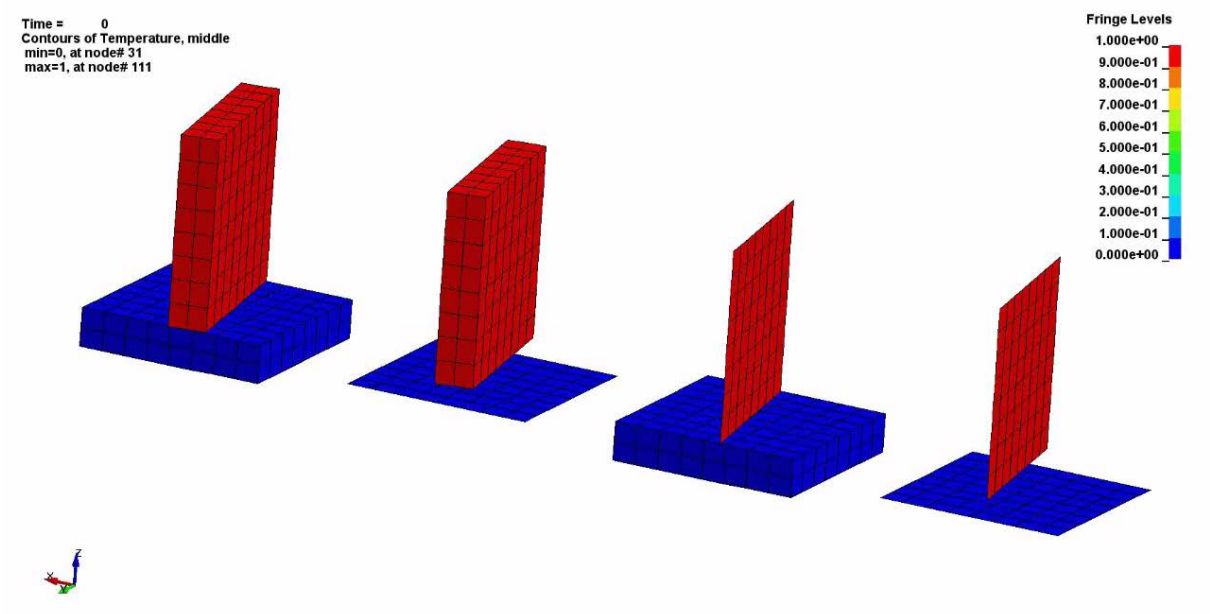

Fig.3: Validation test cases for shell edge thermal contact, initial temperature distribution.

The formulation has been validated using the heat transfer in a T-joint. Four different models are investigated and shown in Fig. 3. In all cases a hot upper part is brought in contact with a cold surface. The resulting temperature fields in Fig. 4 demonstrate that the heat transfer across the edge of the upper part does not change significantly if these parts are modelled with solid or shell elements.

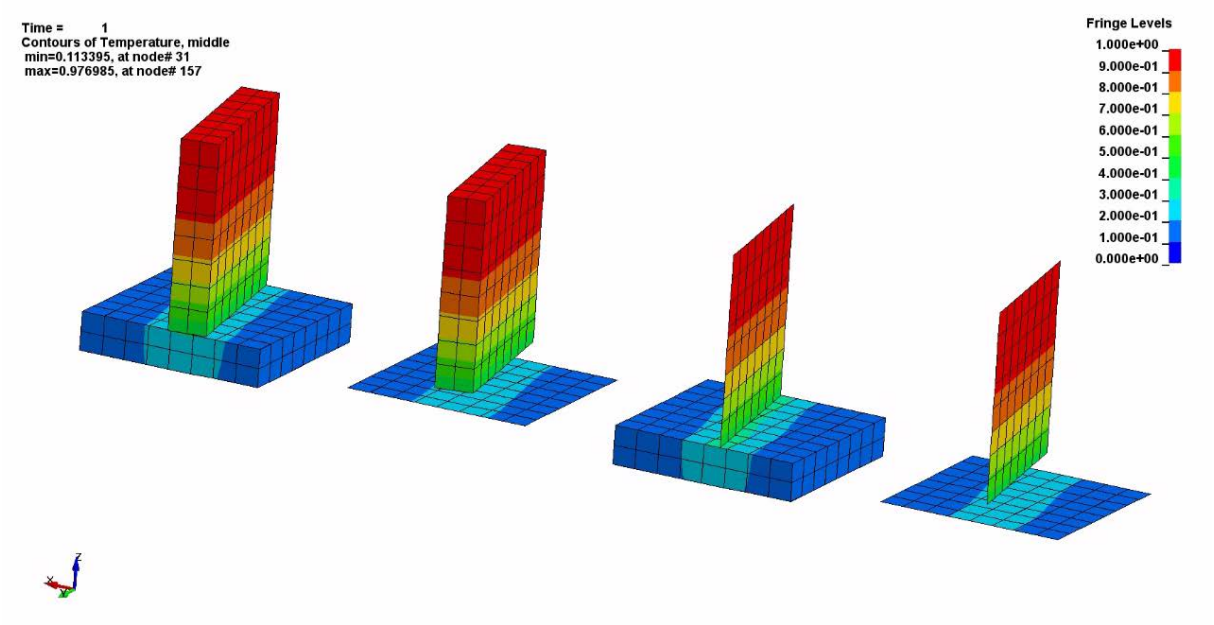

Fig.4: Validation test cases for shell edge thermal contact, resulting temperature distribution.

3.2 Welding contact

Many welding processes used today do not require the presence of a filler material. In those, the materials of the parts to be combined are locally heated up, e.g. by a laser beam. If the melting temperature is exceeded in the contact surface, a strong connection is established and the parts can no longer be separated.

This ghost material approach as discussed above does not seem to be promising. Therefore, a new thermos-mechanical contact formulation has been implemented in LS-DYNA that is defined by the keyword **`*CONTACT_AUTOMATIC_SURFACE_TO_SURFACE_TIED_WELD_THERMAL`**. Mechanically, this contact can switch locally from a sliding contact to a welded, i.e. tied, contact condition. The switch is triggered if the temperature on both surfaces in the contact zone reaches a certain user-defined value. Of course, the contact formulation for the rest of the contact surface is not affected by this switch. Once the welded state of the contact has been reached the contact cannot return to a sliding formulation.

On the thermal side a similar behavior is modelled. The contact keyword introduces an additional parameter to define the thermal conductivity in the welded zone of the contact. In contrast to the mechanical counterpart, the change of the thermal properties is initiated if one side has reached the critical temperature and, thus, has started to melt.

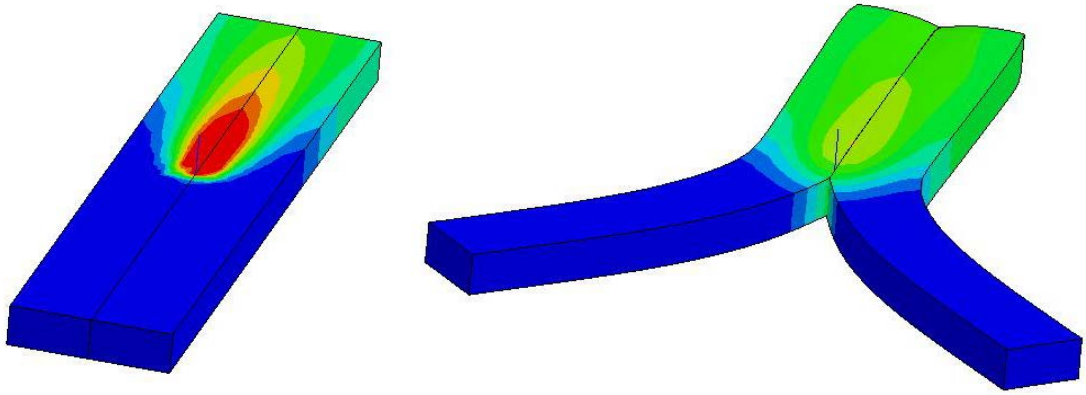

Fig.5: Welding and subsequent loading of a butt weld of two bars. Temperature field at the end of the welding step is shown (left). Loading only results in a separation of the contact areas that have not been affected by the heat.

An example application for this novel feature is the butt weld shown in Fig. 5. As depicted on the left, the weld torch only moves through one half of the contact area. After welding, forces are applied onto two end points of the structure. The deformation shows that the parts can only separate in areas for which the contact has not been affected by the heat source. The tied contact in the welded regions does not allow for separation of the parts.
The new welding functionality has been extended to shell-to-shell contact formulations to enable for example the simulation of laser welding of two or more stacked blanks. A small example of such an application is shown in Fig. 6. Here, a heat source partially welds together two thin blanks. After a short cooling phase forces applied to the non-welded edges pull apart the blanks, showing that the local heating prevents the blanks from separating.

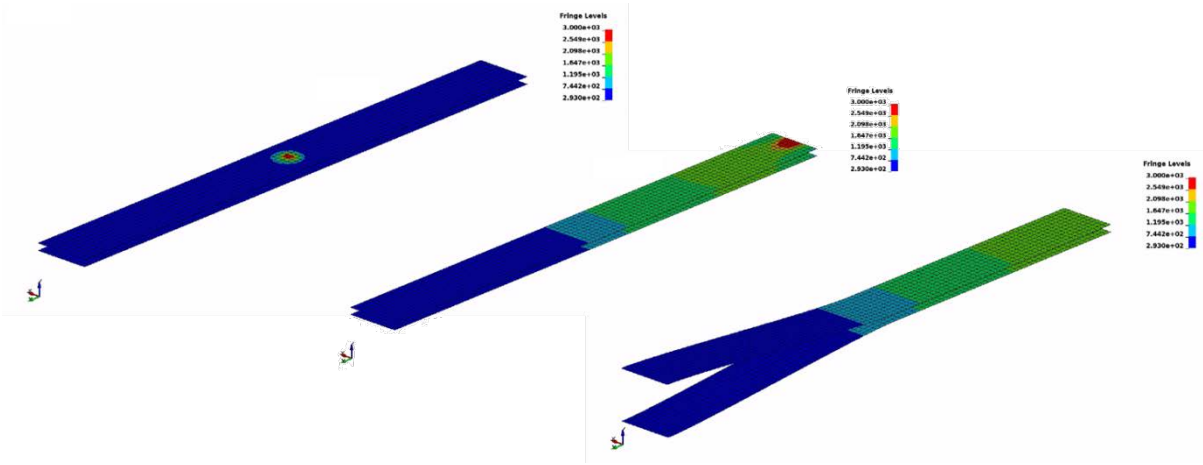

Fig.6: Welding and subsequent loading of two sheet metals. From left to right: Temperature fields at beginning of the welding step, at the end of the welding step and after mechanical loading. Separation prohibited in heat affected contact zones.

New Heat Source Boundary Condition

Drawbacks of available heat source definitions in LS-DYNA have made the creation of a novel model necessary, which is activated by the keyword ***BOUNDARY_THERMAL_WELD_TRAJECTORY**. It is based on the observation that in most line welding processes the weld torch moves with a prescribed velocity on a pre-defined path. In the numerical representation this trajectory of the root of the weld torch is defined by a node set. If those nodes are part of the welded structure, the position of the weld path will be updated automatically with deformation of the structure in a coupled simulation. The velocity of the heat source can either be defined globally or relatively with respect to the motion of the welded structural part.
Besides the position of the root also the orientation of the heat source is to be defined. The new keyword features three different methods to describe it in order to make the input for as many different applications as convenient as possible. As first and simplest option a constant aiming direction can be given by a user-defined vector, but for curved welds as shown in Fig. 3, a constant orientation is probably unrealistic.
One possibility to simulate a varying orientation follows ideas used in ***BOUNDARY_THERMAL_WELD**. A second node set defines a second path and the weld torch is always orientated between this two paths. This approach provides high flexibility but requires a significant pre-processing effort. A remedy could be the third orientation definition implemented into the new boundary condition. For this option the input of a segment set the weld beam is always assumed to be orthogonal to is required. Many applications in fusion welding show parallels to the curved T-joint in Fig. 7. For such applications the third method seems to be the most suitable choice in terms of pre-processing effort and accuracy.
To gain more flexibility and to make variation of process parameters easier, position and orientation can be adapted by time-dependent load curves defining a rotation around the trajectory, a displacement in weld beam direction and a displacement in lateral direction.

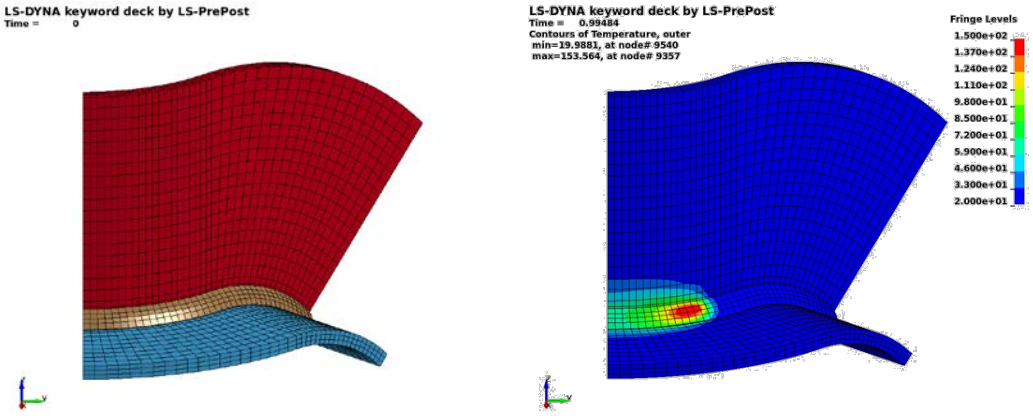

Fig.7: Welding of a curved T-joint. Geometry (left) and temperature field (right)

It is very important to note that due to definitions and functionalities described above, the motion of the weld torch is not necessarily linked to the motion of a structure. Consequently, the novel keyword does not require the presence of a structure solver for modelling a moving heat source but can be employed in thermal-only analyses.

The motion of the heat source frequently becomes the limiting factor for the admissible time step size depending on mesh size and torch velocity. Too large time steps result in an unevenly heating with often unphysically high maximum temperatures. This is due to the fact that by default the solver does not compute intermediate positions and the heat source “jumps” across whole elements. Because the motion of the welding heat source has been transferred from the structure to the thermal solver and is defined by a trajectory, its position can be easily determined at any given point in time. Therefore, a kind of sub-cycling becomes possible, considerably smoothing the temperature distribution and equally important the mesh distortion along the trajectory. Moreover, a thermal dumping can be realized to reduce simulation times.

Although being widely used in industries, the Goldak equivalent heat source [16] might not be the best choice for all applications. Therefore, **`*BOUNDARY_THERMAL_WELD_TRAJCETORY`** enables the user to choose between four different pre-defined equivalent heat source geometries. Of course a Gaussian power density distribution defined on a double ellipsoidal region as proposed by Goldak is one of them. But also constant energy densities on the double ellipsoidal region, on double conical regions or on a frustum are possible. The latter are well-suited for simulation of laser welding processes. The resulting temperature distributions are shown in Fig 8.

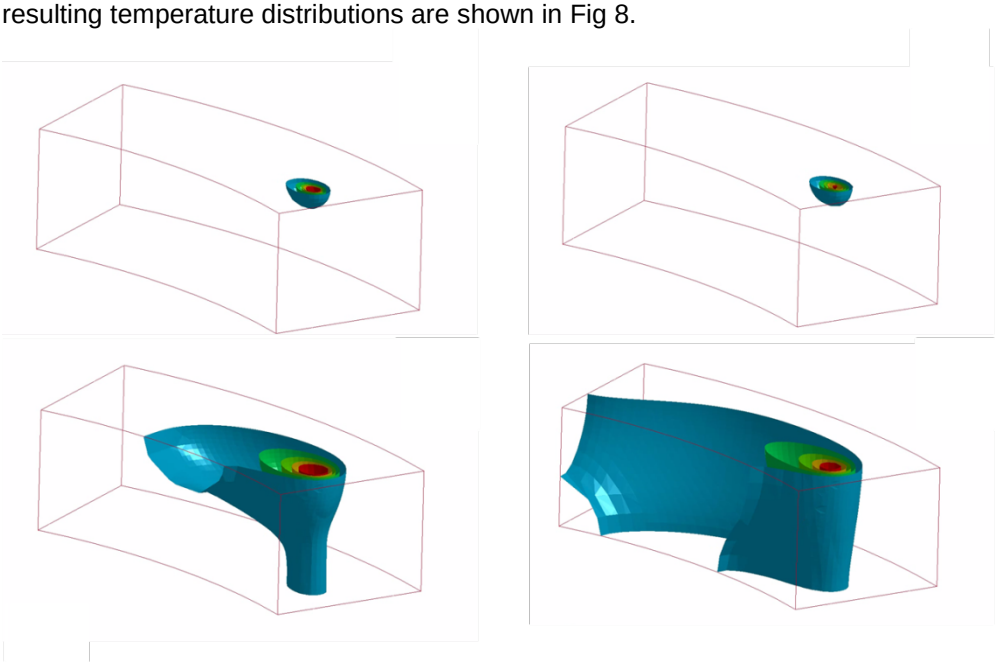

Fig.8: Temperature iso-surfaces for different forms of the equivalent heat source. Bottom line shows results for double ellipsoid with Gaussian (left) and constant (right) energy rate densities, bottom line results for double conical (left) and frustum (right) shapes.

Additionally, the heat source boundary condition can be used to model non-standard heat sources with user-defined energy rate densities. Using the keyword ***DEFINE_FUNCTION** those can be expressed in a local coordinate system moving along the trajectory.
In most cases welding is only one of many links in the process chain. Today it is state of the art to use solid discretizations for welding simulations, whereas most of the other process steps are simulated using shell meshes. The new keyword extends the welding functionality in LS-DYNA to shells to enable an easy transition of data between different process stages. Best accuracy can be obtained by using the thermal thick shell formulation, which enables a linear temperature gradient across the shell thickness of the elements, while any shell formulation implemented in LS-DYNA can be used to solve the mechanical problem.

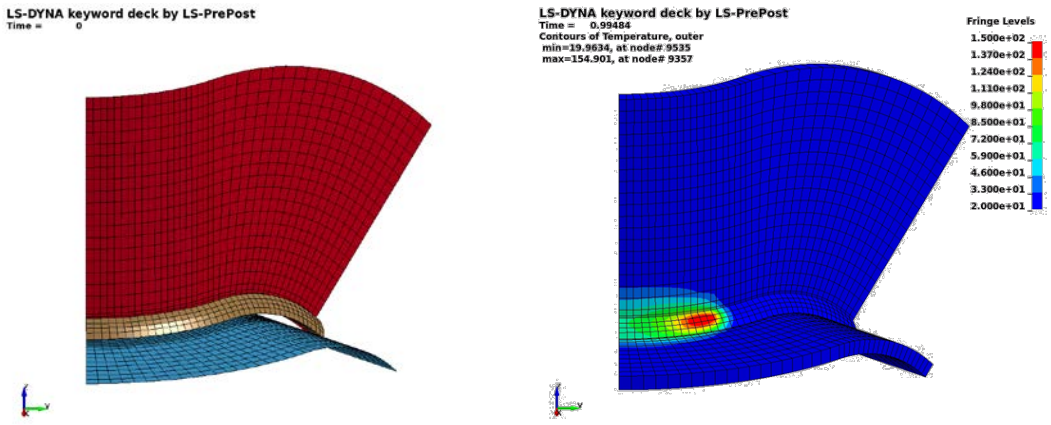

Fig.9: Welding of a curved T-joint discretized with shell elements. Geometry (left) and temperature field (right). Only to visualize the temperature gradients in shell normal direction, the shells are shown as volume elements in post-processing.

Figures 7 and 9 show equivalent solid and shell meshes for a curved T-joint. In both cases the welded parts and the weld seam are connected with a tied contact formulation and the geometry of the weld pool was chosen such that it exceeds the solid discretization of the weld seam. The resulting temperature fields show an excellent agreement. Neglecting the heat input into the shell elements would result in a significant drop of the maximum temperature by almost 20%. This demonstrates that the new implementation has been necessary to simulate weld processes using shell elements.

Literaturverzeichnis

[1] M. Schill and E.-L. Oldenberger, "Simulation of residual deformation from a forming and welding process using LS-DYNA," in *Proc. of 13th International LS-DYNA Conference*, Detroit, 2014.

[2] P. Åkerström und M. Oldenburg, „Austenite decomposition during press hardening of a boron steel – Com-puter simulation and test," *Journal of Materials Processing Technology,* Bd. 174, pp. 399-406, 2006.

[3] P. Åkerström, G. Bergman and M. Oldenburg, "Numerical implementation of a constitutive model for simu-lation of hot forming," *Modeling and Simulation in Materials and Engineering,* vol. 15, pp. 105-119, 2007.

[4] P. Hippchen, A. Lipp, H. Grass, P. Craighero, M. Fleischer und M. Merklein, „Modelling kinetics of phase transformation for the indirect hot stamping process to focus on car body parts with tailored properties," *Journal of Materials Processing Technology,* Bd. 228, pp. 59-67, 2016.

[5] P. Hippchen, M. Merklein, A. Lipp, M. Fleischer, H. Grass and P. Craighero, "Modelling kinetics of phase transformation for the indirect hot stamping process," *Key Engineering Materials,* vol. 549, pp. 108-116, 2013.

[6] P. Lindström, „DNV Platform of Computational Welding Mechanics," in *Proc. Of Int. Inst. Welding 66th Annual Assembly* , 2013.

[7] P. Lindström, L. Josefson, M. Schill und T. Borrvall, „Constitutive Modelling and Finite Element Simulation of Multi Pass Girth Welds," in *Proc. Of NAFEMS NORDIC Conference*, Gothenburg, 2012.

[8] T. Klöppel und T. Loose, „Recent developments for thermo-mechanically coupled simulations in

LS-DYNA with focus on welding processes," in *Proc. of 10th European LS-DYNA Conference*, Wuerzburg, 2015.

[9] M. Koistinen and R. Marburger, "A General Equation Prescribing the Extent of the Austenite-Martensite-Transformation in Pure Iron Carbon-Alloys and Plan Carbon Steels," *Acta Metallurgica,* vol. 7, pp. 59-60, 1959.

[10] M. Fanfoni and M. Tomellini, "The Johnson-Mehl-Avrami-Kolmogorov model: A brief review," *Il Nuovoto Cimento D,* vol. 20, pp. 1171-1182, 1998.

[11] J. Leblond and J. Devaux, "A New Kinetic Model for Anisothermal Metallurgical Transfromations in Steels Including Effect of Austenits Grain Size," *Acta Metallurgica,* vol. 32, pp. 137-146, 1984.

[12] J. Kirkaldy und D. Venugopalan, „Prediction of microstructure and hardenability in low alloy steels," in *Internalional conference on phase transformation in ferrous alloys*, Philadelphia, 1983.

[13] A. Oddy, J. McDill und L. Karlsson, „Microstructural predictions including arbitrary thermal histories, reaustinitization and carbon segregation effects," *Canadian Metallurgical Quarterly,* Bd. 35(3), pp. 275-283, 1996.

[14] T. Klöppel, M. Schill und T. Loose, „Recent Updates for the Heat Transfer Solver in LS-DYNA with focus on computational welding mechanics," in *Proc. of 14th International LS-DYNA Conference*, Detroit, 2016.

[15] J. Leblond, „Mathematical modelling of transformation plasticity in steels ii: Coupling with strain hardening phenomena," *International Journal of Plasticity,* Bd. 5, pp. 573-589, 1989.

[16] J. Goldak, A. Chakravarti und M. Bibby, „A Double Ellipsoid Finite Element Model for Welding Heat Sources," *IIW Doc.No.212-603-85,* 1985.